Japanese Journal of Applied Physics **51** (2012) 09MK05 **REGULAR PAPER**
http://dx.doi.org/10.1143/JJAP.51.09MK05

Hotspot Location Shift in the High-Power Phosphor-Converted White Light-Emitting Diode Packages

Run Hu, Xiaobing Luo*, and Huai Zheng

Thermal Packaging Laboratory, School of Energy and Power Engineering, Huazhong University of Science and Technology, Wuhan 430074, China

Received October 30, 2011; accepted May 12, 2012; published online September 20, 2012

Thermal management of high-power light-emitting diodes (LEDs) plays an important role in determining their optical properties, reliability, and lifetime. In this paper, we present a method to study the temperature field of phosphor-converted LED packages by combining the Monte Carlo optical simulation and finite element simulation together. The temperature field, including the heat generation in both LED chip and phosphor layer, are presented and analyzed. It was found that temperature increased with the increase in phosphor concentration and the hotspot location in remote phosphor-coating packages shifted with the changes in phosphor concentration, while there was no shift in direct phosphor-coating packages. It was concluded that the hotspot location in the high-power phosphor-converted white LED packages depended on phosphor concentrations as well as packaging methods. © 2012 The Japan Society of Applied Physics

1. Introduction

Light-emitting diodes (LEDs) are solid-state light emitters known for their high energy efficiency, long lifetime, design flexibility, and robustness.[1–3] Considered as a strong candidate for the next-generation light sources, high-power LEDs have been developed rapidly in recent years and widely used in our daily life such as vehicle headlamps, traffic lights, landscape lighting, and even indoor fixtures.[4–11] However, the increasing power results in high heat flux generated in high-power LED packages.[12–14] The corresponding high temperature has an obvious negative impact on the optical performance and reliability of LED packages. Firstly, it will weaken the radiative combination and enhance the nonradiative combination of the electrons and holes inside the heterostructure of the p–n junction, and this will reduce internal quantum efficiency and increase heat generation greatly. As a result, the output luminous efficacy degrades. Secondly, it will induce the material property deterioration, local stress, and even delamination, which results in the degradation of reliability and lifetime significantly.[15] Thirdly, since phosphor efficiency decreases exponentially with the increase in phosphor temperature, high temperature is also a critical problem for phosphors.[16–18] Therefore, much effort has been spent on investigating the thermal performance of high-power LED packages as well as phosphors.[19–26] Fan *et al.*[25] compared conventional and thermal-isolated phosphor coatings by both experiments and finite-element simulations. They found that the surface temperature of the thermal-isolated phosphor coating layer was 16.8 °C lower than that of the conventional packaging. Yan *et al.*[26] demonstrated that the temperature of phosphor particles, regardless of the phosphor placement, was always higher than the junction temperature. They found that the temperature of the remote coating phosphor layer was higher than that of the conventional phosphor coating when the phosphor concentration was changed from 30 to 80 wt %. It is discovered that these two results are contrary to each other with regard to whether the temperature of remote coating phosphor was higher. For a blue LED emitter without phosphor coating, the hotspot must be located close to the chip. Therefore, it is intuitionistic that the hotspot location depends on the amount of phosphors.

ITO	100nm
p-GaN	150nm
p-$Al_xGa_{1-x}N$	50nm
MQW	100nm
N-GaN	4μm
Sapphire	100μm
Reflecting layer (Ag)	150nm
Bonding layer (AuSn)	

Fig. 1. (Color online) Typical structure of conventional blue LED chip.

In this study, we investigated the relationship between the hotspot location of LED packages with phosphor concentration. In the Monte Carlo optical simulation, we obtained the heat generation that was accumulated by the optical absorption of the LED chip and the phosphor layer, respectively. The heat was loaded on the finite element model and then the thermal simulation was conducted by the finite element method (FEM). By this method, we compared the hotspot location in the same phosphor-converted white LED packages with two different kinds of phosphor coatings, i.e., the direct phosphor coating and the remote phosphor coating, while varying phosphor concentration. The hotspot location was observed and the temperature fields of the LED packages were presented. Detailed analyses of the temperature fields were presented as well.

2. Simulations

First of all, we must build an accurate GaN-based blue LED chip model. The typical structure of conventional GaN-based blue LED chip is shown in Fig. 1. The thickness and composites of different layers were sketched and the chip size was $1 \times 1\ mm^2$. Luminescencent multi-quantum wells (MQWs) were sandwiched by an n-GaN layer and a heterostructure of p-GaN layer and p-AlGaN layer. A current spreading layer fabricated by indium tin oxide (ITO) and a sapphire substrate were also taken into consideration in the chip model. The top and bottom surfaces of the MQW were set as luminescent surfaces with

*E-mail address: luoxb@mail.hust.edu.cn

 © 2012 The Japan Society of Applied Physics

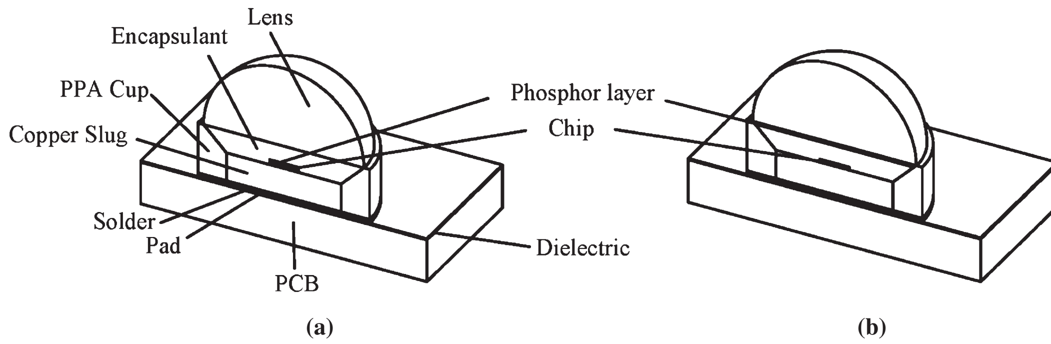

Fig. 2. Half-3D view of white LED packages with (a) direct phosphor coating and (b) remote phosphor coating.

Lambertian light distribution. The absorption coefficients and refractive indices of p-GaN, MQW, and n-GaN were 5, 8, and 5 mm^{-1} and 2.45, 2.54, and 2.42, respectively.[27–29] The reflection coefficient of the reflecting layer (Ag) was set as 0.95. By setting the absorption coefficients and refractive indices of the materials, the optical model of the conventional GaN-based blue LED emitter was successfully achieved.

In this study, we built the same models as those in ref. 26. As shown in Fig. 2, the LED module is mounted on a metal-core-printed circuit board (PCB) for electrical connection and heat dissipation. Inside the LED module, a $1 \times 1\,\mathrm{mm}^2$ blue LED chip is mounted onto a copper slug via die attach adhesive. The copper slug is embedded in a polyphthalamide reflector cup (PPA cup) and bonded onto the PCB via solder. Conventional hemispherical lens and silicone encapsulant are also considered. Figure 2(a) shows the half-3D view of a LED package with direct phosphor coating, where the phosphor layer is coated onto the top of the chip directly; while Fig. 2(b) shows that with remote phosphor coating, where the phosphor layer is separated from the chip by silicone encapsulant. The phosphor layers in both direct coating and remote coating packages are composed of yellow phosphors embedded in a silicone matrix whose thickness was 80 μm and the efficiency was assumed as 70%. The whole simulations consisted of two steps: in the first step, we conducted optical simulation and calculated the heat flux accumulated by the light absorption of both the chip and phosphor layer; in the second step, a FEM model was set up to simulate the temperature field of the LED packages. As for the optical simulation, the color conversion process was achieved by taking account of the absorption of the blue light by the yellow phosphor particles, the re-emission of yellow light, and the scattering of all the light within the phosphor particles and the LED chip multilayer structure. In the simulation, two wavelengths were ray-traced separately, namely 465 and 555 nm, which could represent the blue LED light and the phosphor-converted yellow light, respectively.[27] The wavelength-dependent refractive indices, absorption, and scattering coefficients, which varied with the changes in phosphor concentration,[29,30] played an important role in determining the optical performance of the LED packages and influencing the heat flux accumulated by the chip and phosphor layer. Furthermore, the refractive indices of the silicone encapsulant and polymethylmethacrylate lens were 1.6 and 1.4935 for both wavelengths, respectively. The three-dimensional Monte

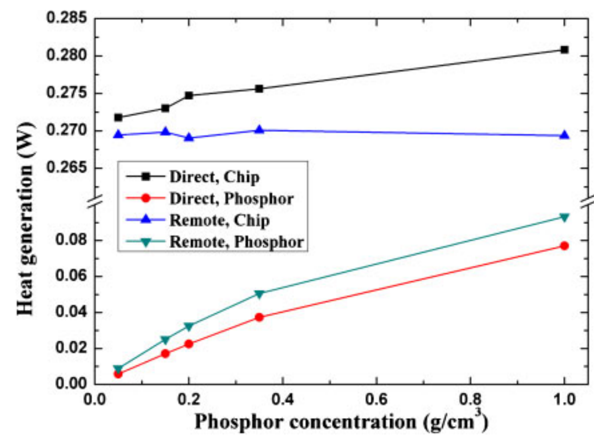

Fig. 3. (Color online) Heat generation of the chip and the phosphor layer with different phosphor coatings.

Carlo ray-tracing simulations were implemented with the commercial software package Tracepro. After finishing the optical simulations, the light flux absorbed by the chip and the phosphor layer was obtained and assumed as the heat load on the FEM model.

In the FEM simulation, only the one-quarter finite element model was considered to simulate the temperature field because of its symmetry. The thermal conductivities of all the material including the phosphor layer were given according to ref. 26. The boundary conditions of the FEM model were also the same as those in ref. 26: forced convection at the bottom surface of the PCB with a heat transfer coefficient of $30\,\mathrm{W/(m^2{\cdot}{}^\circ C)}$, and nature convection on all other surfaces of the LED packages with a heat transfer coefficient of $10\,\mathrm{W/(m^2{\cdot}{}^\circ C)}$. The ambient and initial temperatures were kept at 25 °C.

3. Results and Discussions

The heat generation of the chip and the phosphor layer was accumulated from the absorption loss of the light. Since the phosphor efficiency was assumed as 70%, only 70% of the absorbed blue light was converted into yellow light emission and the remaining 30% was converted to heat. As shown in Fig. 3, it is evident that with the increase in phosphor concentration, the heat generation of both LED packages with two kinds of phosphor coatings increased greatly. The heat generation of the LED chip with direct phosphor coating increased, but the heat generation of the LED chip

 © 2012 The Japan Society of Applied Physics

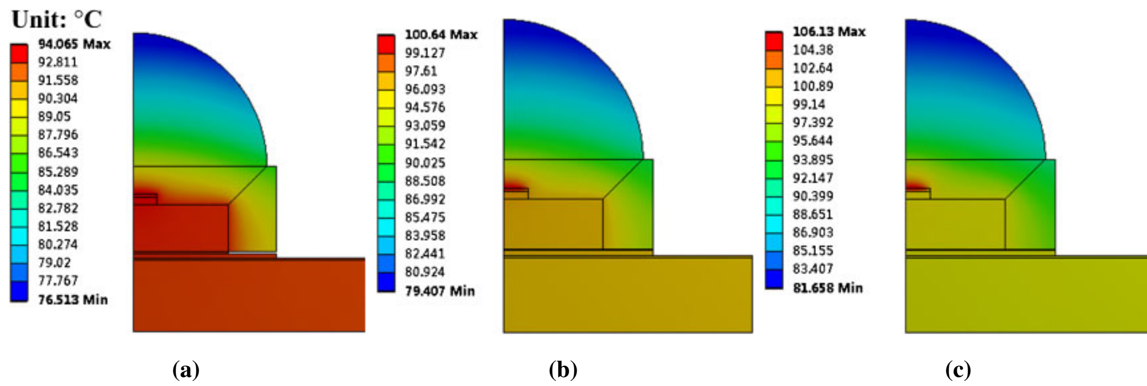

Fig. 4. (Color online) Temperature distribution of the LED package with direct phosphor coating with different phosphor concentrations: (a) 0.05, (b) 0.2, and (c) 0.35 g/cm^3.

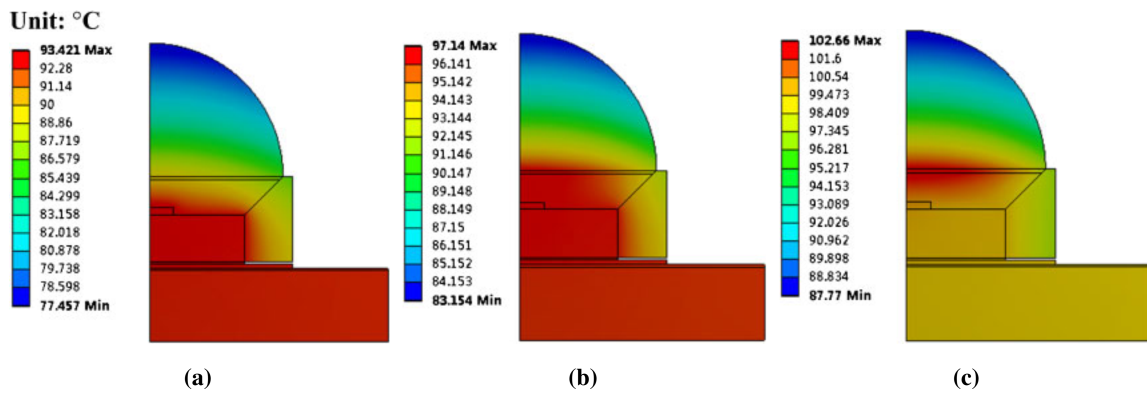

Fig. 5. (Color online) Temperature distribution of the LED package with remote phosphor coating with different phosphor concentrations: (a) 0.05, (b) 0.2, and (c) 0.35 g/cm^3.

with remote phosphor coating almost remained the same. The reasons may be as follows: (1) the larger the phosphor concentration was, the more light would be absorbed by the phosphor; therefore, the heat generation of the phosphors increased greatly; (2) since the phosphor layer was directly coated on the top surface of the chip in the direct coating package, more blue light emanated from the chip would be back-scattered to the chip, which enhanced the heat generation of the chip. Therefore, the heat generation of the chip with direct phosphor coating was larger than that with remote phosphor coating.

The heat generation obtained from the Monte Carlo simulations was loaded on the FEM models and the temperature fields of these two models are shown in Figs. 4 and 5, respectively. The temperature fields were close to the temperature fields in ref. 25, which validated the FEM model used in this study. It was obvious that with the increase in phosphor concentration from 0.05 to 0.35 g/cm^3, the temperatures of the LED packages increased and the hotspot became increasingly obvious. The hotspot location was close to the phosphor layer in Fig. 4 regardless of the increase in phosphor concentration. As shown in Fig. 5, however, there existed a shift of the hotspot location. When the phosphor concentration was low (e.g., 0.05 g/cm^3), the hotspot was located at the chip; when the phosphor concentration increased, the hotspot location shifted to the phosphor layer in the end. The reasons behind this phenomenon may be as follows. (1) The phosphor layer with high concentration generated more heat, as shown in Fig. 3; (2) Since the phosphor layer was separated by the silicone encapsulant, and the thermal conductivity of the silicone encapsulant was very low, the heat generated inside the phosphor layer could hardly be transferred to the ambient air. Therefore, heat was accumulated and the temperature increased greatly as a result.

To quantitatively analyze the above phenomenon, the chip temperature, phosphor temperature, and maximum temperature of the two packages were taken out and shown in Fig. 6. It was demonstrated that with the increase in phosphor concentration, the three temperatures increased regardless of the phosphor coating methods. From Fig. 6(a), it is seen that the chip temperature is lower than phosphor temperature and the maximum temperature curve overlapped with the phosphor temperature curve. It indicated that for the direct phosphor coating, the phosphor layer was the hotspot location despite the changes in phosphor concentration. For the remote phosphor coating, as shown in Fig. 6(b), it is seen that when the phosphor concentration is lower than 0.2 g/cm^3, the chip temperature is higher than the phosphor temperature and the maximum temperature is located close to the chip; when the phosphor concentration exceeds 0.2 g/cm^3, the phosphor temperature is higher than the chip temperature and the maximum temperature is located at the phosphor layer. Therefore, for the remote phosphor coating,

© 2012 The Japan Society of Applied Physics

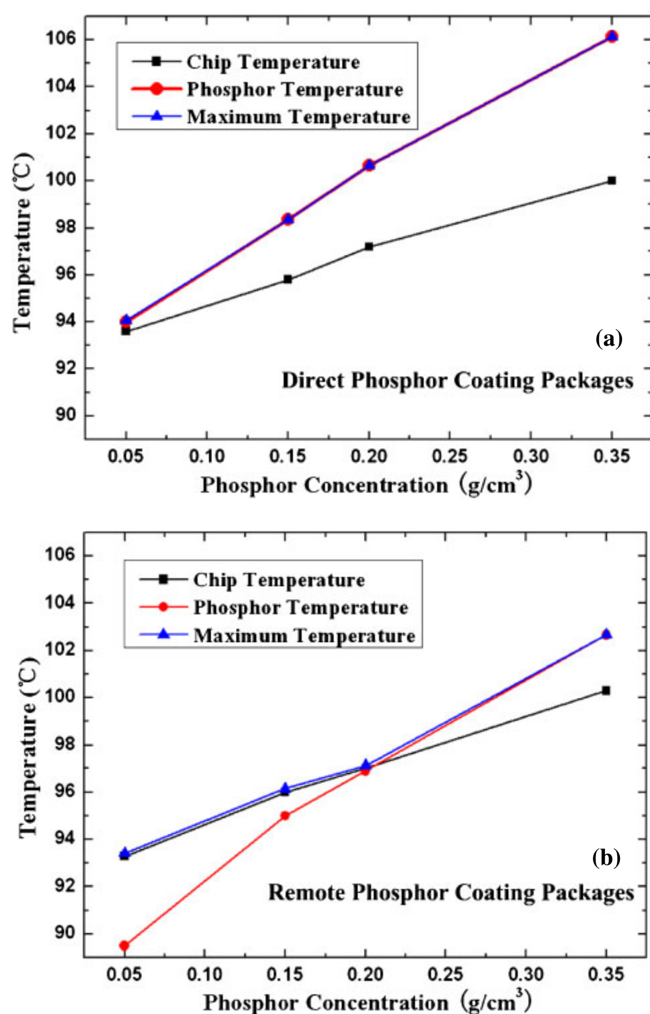

Fig. 6. (Color online) Temperature comparisons with the changes in phosphor concentration of LED packages with (a) direct phosphor coating and (b) remote phosphor coating.

there existed an obvious hotspot location shift. These results agreed with those shown in Figs. 4 and 5.

It is also noted from Fig. 6(b) that the maximum temperature curve did not exactly overlap with the chip temperature curve when the phosphor concentration is lower than 0.2 g/cm^3. This is because the actual maximum temperature was at the silicone encapsulant close to the chip, but not located at the chip exactly owing to the high thermal conductivities of the chip and the PCB.

From Fig. 6, it can also be seen that the temperature of direct phosphor coating package was higher than that of remote phosphor coating. There may be two reasons. The one is that the chip with direct phosphor coating generated more heat, as shown in Fig. 3; The other is that more heat would transfer from the chip to the direct coating phosphor layer since the layer was directly coated on the chip. Therefore, the direct phosphor coating package had higher temperature.

4. Conclusions

In summary, this paper deals with the hotspot location shift in the high-power phosphor-converted white LEDs. By combining optical simulation with FEM simulation, the temperature fields of the LED packages were presented and analyzed. It was found that the hotspot location in the remote phosphor coating packages shifted with the changes in phosphor concentration, while there was no shift in the direct phosphor coating packages. In summary, the hotspot location depended on phosphor concentration as well as packaging methods.

Acknowledgements

This work was supported in part by the Major State Basic Research Development Program of China (973 Program: No. 2011CB013105), and in part by National High Technology Research and Development Program of China (863 Program: No. 2011AA03A109).

1) S. Pimputkar, J. S. Speck, S. P. Denbaars, and S. Nakamura: Nat. Photonics **3** (2009) 180.
2) E. F. Schubert and J. K. Kim: Science **308** (2005) 1274.
3) S. Liu and X. B. Luo: *LED Packaging for Lighting Applications: Design, Manufacturing and Testing* (Wiley, Singapore, 2011) Chap. 3.
4) Z. Y. Liu, S. Liu, K. Wang, and X. B. Luo: Front. Optoelectron. **2** (2009) 119.
5) H. Zheng, X. B. Luo, R. Hu, B. Cao, X. Fu, Y. M. Wang, and S. Liu: Opt. Express **20** (2012) 5092.
6) R. Hu, X. B. Luo, and S. Liu: IEEE Photonics Technol. Lett. **23** (2011) 1673.
7) R. Hu, X. B. Luo, H. Feng, and S. Liu: J. Lumin. **132** (2012) 1252.
8) Y. Narukawa, J. Narita, T. Sakamoto, K. Deguchi, T. Yamada, and T. Mukai: Jpn. J. Appl. Phys. **45** (2006) L1084.
9) B. R. Yang, K. H. Liu, and H. P. D. Shieh: Jpn. J. Appl. Phys. **46** (2007) 182.
10) D. Feng, J. Yoo, K. Nagatani, W. Kim, and H. C. Kim: Jpn. J. Appl. Phys. **46** (2007) 563.
11) Y. Narukawa, I. Niki, K. Izuno, M. Yamada, Y. Murazaki, and T. Mukai: Jpn. J. Appl. Phys. **41** (2002) L371.
12) Q. Chen, X. B. Luo, S. J. Zhou, and S. Liu: Rev. Sci. Instrum. **82** (2011) 084904.
13) X. B. Luo, W. Xiong, T. Cheng, and S. Liu: IET Optoelectron. **3** (2009) 225.
14) J. R. Grandusky, S. R. Gibb, M. C. Mendrick, C. Moe, M. Wraback, and L. J. Schowalter: Appl. Phys. Express **4** (2011) 082101.
15) E. Fred Schubert: *Light Emitting Diode* (Cambridge University Press, New York, 2006) 2nd ed., Chap. 2.
16) M. Zachau, D. Becker, D. Berben, T. Fiedler, F. Jermann, and F. Zwaschka: Proc. SPIE **6910** (2008) 691010.
17) P. F. Smet, A. B. Parmentier, and D. Poelman: J. Electrochem. Soc. **158** (2011) R37.
18) M. Arik, S. Weaver, A. Setlur, and D. Haitko: Proc. IMECE, 2005, p. 79330.
19) Y. B. Chen, M. L. Gong, G. Wang, and Q. Su: Appl. Phys. Lett. **91** (2007) 071117.
20) S. W. Allison, J. R. Buczyna, R. A. Hansel, D. G. Walker, and G. T. Gillies: J. Appl. Phys. **105** (2009) 036105.
21) P. Vitta, P. Pobedinskas, and A. Zukauskas: IEEE Photonics Technol. Lett. **19** (2007) 399.
22) X. B. Luo, B. Wu, and S. Liu: IEEE Trans. Device Mater. Reliab. **10** (2010) 182.
23) T. Cheng, X. B. Luo, S. Y. Huang, and S. Liu: Int. J. Therm. Sci. **49** (2010) 196.
24) X. B. Luo, R. Hu, T. H. Guo, X. L. Zhu, W. Chen, Z. M. Mao, and S. Liu: 60th ECTC2010, 2010, p. 1347.
25) B. F. Fan, H. Wu, Y. Zhao, Y. L. Xian, and G. Wang: IEEE Photonics Technol. Lett. **19** (2007) 1121.
26) B. Yan, N. T. Tran, J. P. You, and F. G. Shi: IEEE Photonics Technol. Lett. **23** (2011) 555.
27) Z. Y. Liu, K. Wang, X. B. Luo, and S. Liu: Opt. Express **18** (2010) 9398.
28) Z. Y. Liu, S. Liu, K. Wang, and X. B. Luo: IEEE Photonics Technol. Lett. **20** (2008) 2027.
29) Z. Y. Liu, S. Liu, K. Wang, and X. B. Luo: Appl. Opt. **49** (2010) 247.
30) R. Hu, X. B. Luo, H. Zheng, Q. Zong, Z. Q. Gan, B. L. Wu, and S. Liu: Opt. Express **20** (2012) 13727.

© 2012 The Japan Society of Applied Physics